Optical model description of the neutron interaction with ^{116}Sn and ^{120}Sn over a wide energy range

P. P. Guss,* R. C. Byrd,† C. R. Howell, R. S. Pedroni,‡ G. Tungate,§ and R. L. Walter
Department of Physics, Duke University, Durham, North Carolina 27706
and Triangle Universities Nuclear Laboratory, Durham, North Carolina 27706

J. P. Delaroche
Service de Physique et Techniques Nucléaire, Centre d'Études de Bruyères-le-Châtel, 97680 Bruyères-le-Châtel, France
(Received 6 September 1988)

Differential cross sections for neutron elastic scattering and inelastic scattering to the first 2^+ and 3^- excited states have been measured at 10, 14, and 17 MeV for ^{120}Sn and at 10 and 14 MeV for ^{116}Sn. Analyzing powers have also been measured at 10 and 14 MeV for elastic scattering from both isotopes and at 10 MeV for inelastic scattering from ^{120}Sn. These data have been analyzed in the framework of the coupled-channels formalism for vibrational nuclei. Previously reported neutron scattering measurements performed below 25 MeV, along with total cross-section measurements from 10 keV to 100 MeV, and *s*- and *p*-wave strength functions were also considered in the analysis in order to place additional constraints on the optical potential parameters. Neutron scattering deformations have been deduced for the quadrupole and octupole vibrations. These deformations have been compared with those derived from earlier (n,n') and (p,p') scattering measurements which were reanalyzed in the present work.

I. INTRODUCTION

In order to achieve a better understanding of neutron scattering in the $A=120$ region and to investigate the competition between the surface and volume absorption, differential cross sections $\sigma(\theta)$ and analyzing powers $A_y(\theta)$ for neutron scattering from ^{116,120}Sn have been measured at the Triangle Universities Nuclear Laboratory (TUNL). These measurements provide the only polarization data for neutron scattering from enriched isotopes in this region of the periodic table. The description of this type of data places severe constraints on proposed nuclear models and helps to reduce the uncertainties in the parametrization of the nucleon-nucleus interaction. Although the emphasis of the experiments was to obtain high accuracy $\sigma(\theta)$ and $A_y(\theta)$ data for elastic scattering, data for inelastic scattering were also obtained. The experiments covered the energy range between 10 and 17 MeV, the energy region where the volume absorption starts to become significant.

The new scattering data have been combined with earlier (n,n) and (n,n') differential cross section data,[1,2] with (p,p) and (p,p') scattering measurements[3] for ^{116,120}Sn at 16 MeV, with the low-energy neutron scattering parameters[4] and with total cross section (σ_T) measurements[5,6] in a comprehensive coupled-channels (CC) analysis. The primary aim of this analysis has been to determine the energy dependence of the different terms of the nucleon-nucleus optical model potential for nucleon scattering from Sn, primarily over the entire 10 keV to 30 MeV energy range, a range where many constraints can now be placed on the deformed central potentials and on the spin-orbit potential. Particular emphasis has been placed on investigating the energy dependences of the strengths W_D and W_V of the surface and volume absorption potentials, respectively, which have been explored up to $E=100$ MeV by optimizing the fit to available σ_T data.[5,6] Through the analysis of the $A_y(\theta)$ data for (n,n') scattering, deformation lengths δ_{SO} for the spin-orbit potential have been extracted for comparison to values found earlier for (n,n') scattering from other nuclei and also for investigating the conjecture of Raynal[7] that proton closed-shell nuclei should have anomalously large values for δ_{SO}.

Earlier neutron measurements of scattering and reactions for Sn isotopes have revealed some interesting features on the interaction between neutrons with these nuclei, which are characterized by having a closed proton shell. In particular, for these nuclei the measured *s*-wave strength functions S_0 drop to the deepest minimum observed[4] over the wide range of mass beyond $A=40$. Although it is generally accepted that this deep minimum in $S_0(A)$ values is related[8] to the shell closure at $Z=50$, the pioneering optical model (OM) studies[9] met with only limited success in explaining the S_0 behavior in the vicinity of $A=120$. More recently, Newstead *et al.*[10] performed OM calculations designed to explain the S_0 values measured for the Sn (and Te) isotopic chain. They had some success by assuming that at low incident energy ($E\sim 10$ keV) both the real part V and the surface imaginary part W_D of the OM potential contain the usual symmetry terms:

$$V=V_0-V_1\epsilon, \quad W_D=W_0-W_{D1}\epsilon ,$$

where $\epsilon=(N-Z)/A$. The strengths derived were

$V_1 \sim 25$ MeV and $W_{D1} \sim 45$ MeV. While this value for V_1 is in the vicinity of that commonly accepted,[11,12] a value of 45 MeV for W_{D1} is abnormally large since it is believed that the relation $W_{D1}/V_1 \sim \frac{1}{2}$ is generally true. Successive DWBA analyses[1,2] of (n,n') scattering data for ^{116,124}Sn at 11 and 24 MeV indicated that W_{D1} has a "normal" value of about 12 MeV, that is, a value consistent with those obtained for a range of nuclei in (p,n) analyses for energies above 20 MeV. (For example, see Ref. 13.) This DWBA value also appears to be more realistic than the value $W_{D1} \sim 23$ MeV found in an early DWBA analysis of (p,p') scattering from Sn isotopes.[3] One goal of the present work was to extend these earlier studies to the CC method of analysis, using a larger data base and one which included for the first time $A_y(\theta)$ data for the neutron channel, in order to see if the complete data set, including the strength functions, could be explained with conventional values for V_1 and W_1.

The present data are also important for other types of nuclear model investigations. For example, considerable success has been achieved with microscopic models of nucleon-nucleus scattering processes, where the models are based on the nuclear matter approach using realistic nucleon-nucleon forces. Examples for elastic scattering of neutrons from ^{208}Pb, ^{93}Nb, and ^{54}Fe(n,n) can be found in Refs. 14, 15, and 16, respectively. A detailed study of microscopic spherical OM calculations for elastic scattering from Sn, including the present data, is currently underway by one of us (R.L.W.) in collaboration with Hansen and Dietrich of Lawrence Livermore National Laboratory (LLNL), and this work will be described in a separate report. Secondly, neutron scattering models which include the dispersion relation to connect the absorptive part of the optical potential to the real part are beginning to solidify,[17] in particular for neutron scattering from ^{40}Ca and ^{208}Pb. One very recent paper[18] on ^{40}Ca describes an extension of the dispersion relation calculations to the coupled-channels formalism. Such calculations need to be extended to other nuclei; the present data for Sn isotopes will be valuable for studying nucleon scattering from nuclei near $A=120$, but additional isotopic data at more energies than are presently available would be helpful in drawing convincing conclusions. We did not attempt to include the dispersion relation, nor search for energy-dependent geometries at the lower energies (which reflect dispersion corrections); this decision was made in part because we elected to avoid the region where compound-nucleus scattering adds additional complications to the problem.

The present paper is organized in the following manner. In Sec. II the experimental setup and data reduction technique are described. The CC analysis of the neutron scattering and reaction measurements is presented in Sec. III. Quadrupole and octupole deformation parameters deduced in Sec. III from (n,n') data are compared in Sec. IV with those from (p,p') scattering measurements[3] that were reanalyzed in the present work.

A preliminary report on the inelastic scattering data for $A_y(\theta)$ has been included in a previous Rapid Communication.[19] The present calculations for Sn supersede those shown in Ref. 19, although the conclusions presented there are not altered. Furthermore, the present data and calculations supersede the work reported in the dissertation[20] of one of the present authors (P.P.G.). We specifically note that the data reported for the Sn isotopes in Ref. 20 are in error because incorrect densities for the Sn scattering samples were used in determining the multiple scattering and attenuation corrections.

II. EXPERIMENTAL ARRANGEMENT AND DATA HANDLING PROCEDURES

For the $\sigma(\theta)$ measurements the neutron time-of-flight facility at the tandem Van de Graaff Laboratory at TUNL was employed. The setup was similar to that described in previous papers.[21,22] The ^{2}H$(d,n)^3$He reaction was used as the source of neutrons. After accounting for the energy loss in the deuterium gas and the averaging over the angle subtended by the scatterer, the average neutron energies for the measurements were 9.95, 13.99, and 16.90 MeV with respective energy spreads of 0.14, 0.10, and 0.09 MeV. Isotopically enriched cylindrical metallic samples of ^{116}Sn and ^{120}Sn (96% and 98%, respectively) having masses of 43 and 45 g were used.

All the measurements have been corrected for geometry and multiple scattering effects using the TUNL code EFFIGY. At each energy absolute normalization is obtained by measuring yields for ^{1}H$(n,n)^1$H scattering from a calibrated polyethylene scatterer. An overall normalization error of about 4% is attributed to this method. For the elastic-scattering data the relative errors were typically about 2–4 %, and are too small to be seen in our illustrations in Sec. III.

The overall time-of-flight (TOF) resolution of about 2 ns was inadequate for accurate determination of the (n,n') yields at forward scattering angles where the elastic-scattering cross section is relatively large. At the other angles the greatest error in extracting values for (n,n') scattering was the uncertainty in the background level in the TOF spectra; the uncertainties for the (n,n') scattering data are indicated by the error bars shown in Sec. III. Tables of the data along with the assigned uncertainties and Legendre polynomial coefficients for describing $\sigma(\theta)$ have been submitted to the National Nuclear Data Center (NNDC) at BNL.

The $A_y(\theta)$ data were obtained using the same time-of-flight spectrometer. The pulsed and polarized neutron beam was produced with a pulsed and polarized deuteron beam[23] through the polarization transfer reaction[24] ^{2}H$(\vec{d},\vec{n})^3$He. The deuteron beam polarization was determined using the quench-ratio method, as in Ref. 24. The polarization of the neutron beam was typically 0.55. The two calibrated neutron detectors used in the $\sigma(\theta)$ experiment were employed to measure the yields simultaneously on the left and right sides of the incident neutron beam axis. In order to improve the counting rate, the deuterium gas pressure and the cell length were both doubled, resulting in overall neutron energy spreads of 0.53 MeV and 0.49 MeV, respectively, for the average incident neutron energies of 9.90 MeV and 13.89 MeV.

The $A_y(\theta)$ data were corrected for multiple scattering up to third order using the TUNL code JANE, which is a

modified version of the unpublished code that originated with Woye and Tornow at Tübingen. At 9.9 MeV a few data points for inelastic scattering from ^{120}Sn were obtained in extra long runs in order to obtain sufficient statistics to be significant in determining structure in $A_y(\theta)$. The $A_y(\theta)$ data are illustrated in Sec. III. The error bars shown include all known uncertainties, except for a 3% normalization uncertainty due to the inaccuracy in our knowledge of the polarization transfer coefficient[24] for ^{2}H($\vec{d},\vec{n}$)^{3}He. Tables of the $A_y(\theta)$ data, along with associated Legendre polynomial coefficients for the fit to the product $A_y(\theta)\sigma(\theta)$, have been sent to NNDC.

III. DEFORMED NEUTRON OPTICAL POTENTIAL

A. Method

The general method used here to determine the best overall energy- and isospin-dependent deformed optical potential has been described previously;[25] only a brief description will be given here. Prior to initiating CC calculations, it was necessary to decide which excited states should be included in the coupling basis. This issue was raised because the first 3^- state of each isotope lies in the vicinity of several excited states[26] which were not resolved in the present measurements. In order to perform manageable CC calculations, it was decided to consider explicitly those excited states which appear to be the most collective ones in high-resolution (p,p') scattering measurements.[27] These states are graphed in the simplified level schemes shown for ^{116,120}Sn in Fig. 1. Therefore, the coupling scheme adopted for the present study was $(0^+,2^+,3^-,4^+,5^-)$.

B. Analysis

Although we knew that the Sn nuclei that have even A are not simple vibrators,[28] it was decided to described the excited states under consideration as harmonic vibrations of spherical nuclei. This assumption seems justified for the first 2^+ state for which the measured quadrupole moment $Q(2^+)$ is nearly zero through the entire isotopic Sn chain.[29]

The deformed optical potential assumed throughout the present work may be expressed as

$$
\begin{aligned}
U(\mathbf{r}) = & -(V+iW_V)f(r,a_V,R_V) \\
& +4ia_D W_D \frac{d}{dr} f(r,a_D,R_D) \\
& -2i\lambda_\pi^2 V_{\mathrm{SO}} \nabla f(r,a_{\mathrm{SO}},R_{\mathrm{SO}}) \times \nabla \cdot \mathbf{s} \\
& +2i\lambda_\pi^2 W_{\mathrm{SO}} \frac{1}{r}\frac{d}{dr} f(r,a_{W_{\mathrm{SO}}},R_{W_{\mathrm{SO}}}) \mathbf{l}\cdot\mathbf{s} \ , \qquad (1)
\end{aligned}
$$

where the form factor f is of a Woods-Saxon type:

$$f(r,a_i,R_i) = \{1+\exp[(r-R_i)/a_i]\}^{-1} \ ,$$

with

$$R_i = r_i A^{1/3}\left[1+\sum_{\lambda\mu}\alpha^i_{\lambda\mu}Y_{\lambda\mu}\right] . \qquad (2)$$

Here R_i is the potential radius expressed in the center-of-mass coordinates of the system. In Eq. (2) the multipolarity λ runs over the values $\lambda=2$, 3, 4, and 5, and the multipole operators $\alpha^i_{\lambda\mu}$ are expressed in terms of vibration amplitudes β^i_λ, as defined in Ref. 30. The third term in Eq. (1) represents the full Thomas form of the spin-orbit (SO) interaction.[31] The last term in Eq. (1) represents an imaginary SO potential. For the calculations presented here, W_{SO} is set to zero; the significance of this choice is discussed briefly in Sec. V.

As in our previous publications,[11,19,32,33] the deformation lengths ($\delta^i_\lambda=\beta^i_\lambda r_i A^{1/3}$) of the central potential terms were constrained to have identical values $\delta_{\lambda c}$ for each multipolarity. For instance, the symbol δ_{2c} will represent the deformation length of the central potential for a quadrupole vibration. The deformation lengths δ_{4c} and δ_{5c} adopted here are those inferred from a (p,p') scattering analysis.[27] The free parameters associated with vibrations are thus δ_{2c} and δ_{3c}. Eventually, the deformation length $\delta_{\lambda\mathrm{SO}}$ for the real SO potential were permitted to differ from the respective $\delta_{\lambda c}$ values. Complex coupling form factors for the central terms of $U(\mathbf{r})$ were assumed in the CC calculations, which were performed using the code ECIS79 of Raynal.[34]

In elastic scattering the $A_y(\theta)$ at extremely forward angles is strongly affected by the Mott-Schwinger (MS) interaction.[35] This interaction is not incorporated in ECIS79, and was neglected here. The magnitude of the effect on $A_y(\theta)$ was investigated using a spherical optical model code[33] in which the MS interaction could be turned on and off, and for the angular region where present data were obtained, corrections for this effect are indeed small. For inelastic scattering possible effects of the MS interaction are also believed to be small.

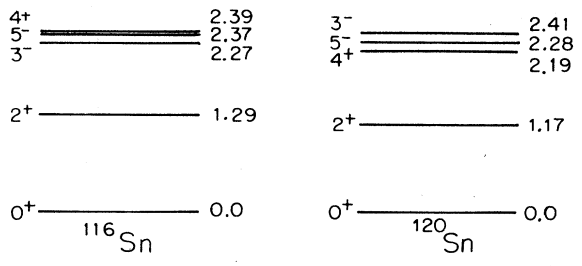

FIG. 1. Simplified level schemes for ^{116,120}Sn. The spins, parities, and excitation energies (in MeV) are taken from Ref. 26.

C. Results

The optimum values found for the potential and deformation parameters are listed in Tables I and II. As expected, the fit to the s- and p-wave strength functions (S_0 and S_1, respectively) requires small values ($W_D<2$ MeV) for the imaginary surface potential depth. Using the potential parameters given in Tables I and II, the s-wave strength function and potential radius R' calculated at 10 keV incident energy for ^{116}Sn are 0.22×10^{-4} and 5.68 fm

TABLE I. Neutron optical potential parameters assumed in the present CC analysis. Incident energy (E) and potential well depths (V, W_D, W_V, V_{SO}) are in MeV. Radii and diffusenesses are in fm and $\epsilon=(N-Z)/A$. Relativistic kinematics used for $E>30$ MeV. The estimated uncertainties attached to $V_1\sim 21$ MeV and $W_{D1}\sim 16$ MeV are 10% and 25%, respectively.

$V=51.97-20.83\epsilon-0.22E$	(0.0 MeV $<E<$ 100 MeV)
$W_D=3.29-15.97\epsilon+1.71\sqrt{E}$	(0.0 MeV $<E\leq$ 13 MeV)
$W_D=9.45-15.97\epsilon-0.08(E-13)$	(13 MeV $\leq E<$ 100 MeV)
$W_V=0.0$	(0.0 MeV $<E\leq$ 13 MeV)
$W_V=0.13(E-13)$	(13 MeV $\leq E<$ 100 MeV)
$V_{SO}=6.50-0.015E$	(0.0 MeV $<E<$ 100 MeV)
$r_V=1.23$, $r_D=1.25$, $r_{so}=1.12$	
$a_V=0.66$, $a_D=0.54$, $a_{so}=0.50$	

compared, respectively, to the experimental values[4] of $(0.26\pm0.05)\times10^{-4}$ and (6.2 ± 0.2) fm, and for ^{120}Sn are 0.15×10^{-4} and 5.65 fm compared, respectively, to $(0.14\pm0.02)\times10^{-4}$ (Ref. 36) and (6.5 ± 0.2) fm (Ref. 4). At the same incident energy, the calculated S_1 value is 3.60×10^{-4} for ^{116}Sn and 2.74×10^{-4} for ^{120}Sn compared to the experimental value[36] of $(2.1\pm0.2)\times10^{-4}$. In summary, except for the p-wave strength functions where the values derived from experiments fall an average of 30% below the calculated values, there is good agreement between the data and calculations for the low-energy neutron scattering parameters. Overall the agreement is quite good, and we note that these results were obtained with an acceptable value for W_{D1} of 16 MeV.

The energy dependence for $W_D(E)$ is given in Table I. In order to get the good agreement between the CC calculations and the low-energy parameters discussed above, as well as with the angular distributions measured at incident energies above 10 MeV, the potential depth $W_D(E)$ is required to increase rapidly in the interval 10 keV $<E\leq 10$ MeV. This behavior is obtained by assuming that $W_D(E)$ increases as $\sqrt{E}$ in this energy domain.

The predictions obtained for $\sigma(\theta)$ are compared with the present and earlier[1,2] measurements for the ground states and the first 2^+ and 3^- states of ^{116,120}Sn in Figs. 2–4. The various curves are intended to illustrate how variations assumed in the deformation lengths of the SO potential effect the CC predictions for $\sigma(\theta)$. In Fig. 5 we show how contributions from individual collective states add up in the CC calculations to form the 10-MeV cross section for the unresolved multiplet in the vicinity of the 3^- state of ^{120}Sn. Similar relative contributions are obtained at 10 MeV for ^{116}Sn and for both isotopes at incident energies between 10 and 24 MeV. Figure 6 shows a comparison between CC predictions and the present and earlier[37] measurements for $A_y(\theta)$. In this figure the sensitivity to varying $\delta_{\lambda SO}$ is illustrated, as it also was in Figs. 2–4. The calculations for $A_y(\theta)$ for inelastic scattering are more sensitive to the value of $\delta_{\lambda SO}$ than those for elastic scattering. From the curves for $A_y(\theta)$ for ^{120}Sn(n,n') in Fig. 6 it is clear that the best overall description would occur when both $\delta_{2SO}\cong 1.2\delta_{2c}$ and $\delta_{3SO}\cong 1.2\delta_{3c}$, although values ranging from about 0.9 to 1.4 might be acceptable. This result is in agreement with our preliminary findings.[19] More $A_y(\theta)$ data are required to draw firm conclusions on $\delta_{\lambda SO}$ for ^{116}Sn. Nevertheless, it can be said that a satisfactory overall description of the $\sigma(\theta)$ and $A_y(\theta)$ measurements is achieved up to 24 MeV, except for the $A_y(\theta)$ for elastic scattering at 10 MeV for $45°<\theta<75°$.

The calculation for $\sigma_T(E)$ is compared to published data in Fig. 7. The yet unpublished $\sigma_T(E)$ measurements[38] from 4 to 80 MeV, which are not shown in Fig. 7, are in excellent agreement with the calculation. We note that the calculated values shown in Fig. 7 for the energy range from 250 keV to 2 MeV systematically lay about 6% higher than the data reported in Ref. 6. A possible source for this discrepancy may be our neglect of the dispersion relation mentioned in Sec. I. [A simple check

TABLE II. Neutron and proton multipole ($\lambda=2,3$) deformation parameters ($\beta^V_{nn'}, \beta^V_{pp'}$) assumed for ^{116}Sn and ^{120}Sn, and related deformation lengths. The Coulomb radius is $R_C=1.20A^{1/3}$ (fm). For $\lambda=2$ and 3 the uncertainties on $\delta_{pp'}$ and $\delta_{nn'}$ values are typically 6% and 10%, respectively.

Reaction	Energy (MeV)	λ	Deformation	Deformation length (fm)	Nuclide
(n,n')	0–24	2	$\beta^V_{nn'}=0.110$	$\delta_{nn'}=0.660$	^{116}Sn
			$\beta^V_{nn'}=0.100$	$\delta_{nn'}=0.607$	^{120}Sn
		3	$\beta^V_{nn'}=0.160$	$\delta_{nn'}=0.960$	^{116}Sn
			$\beta^V_{nn'}=0.150$	$\delta_{nn'}=0.910$	^{120}Sn
(p,p')	16	2	$\beta^V_{pp'}=0.120$	$\delta_{pp'}=0.720$	^{116}Sn
			$\beta^V_{pp'}=0.115$	$\delta_{pp'}=0.697$	^{120}Sn
		3	$\beta^V_{pp'}=0.165$	$\delta_{pp'}=0.990$	^{116}Sn
			$\beta^V_{pp'}=0.160$	$\delta_{pp'}=0.971$	^{120}Sn

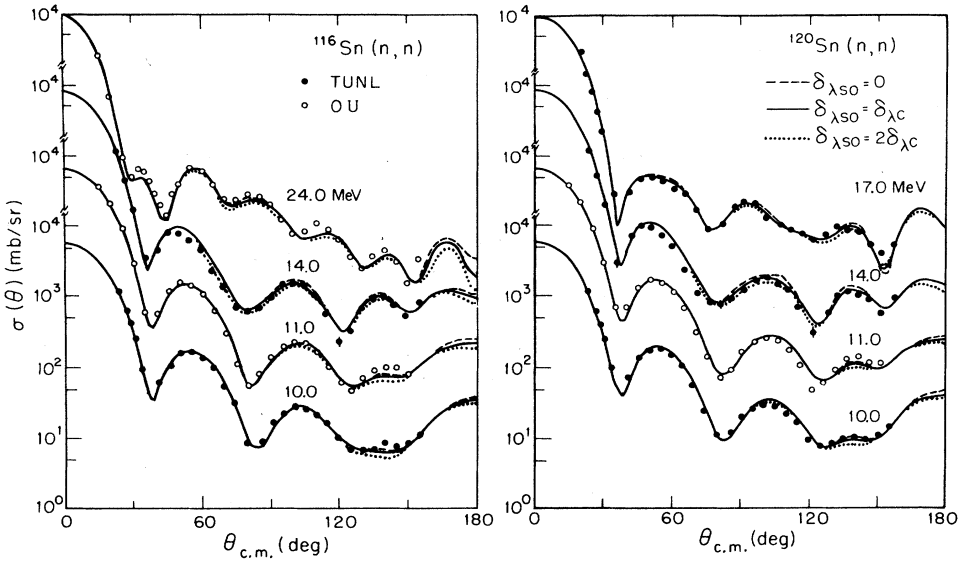

FIG. 2. Differential cross sections for neutron elastic scattering from ^{116}Sn and ^{120}Sn. The curves represent coupled-channels calculations in which the deformation lengths of the deformed spin-orbit potential are varied. The filled circles are the present measurements. The open circles are measurements from Refs. 1 and 2.

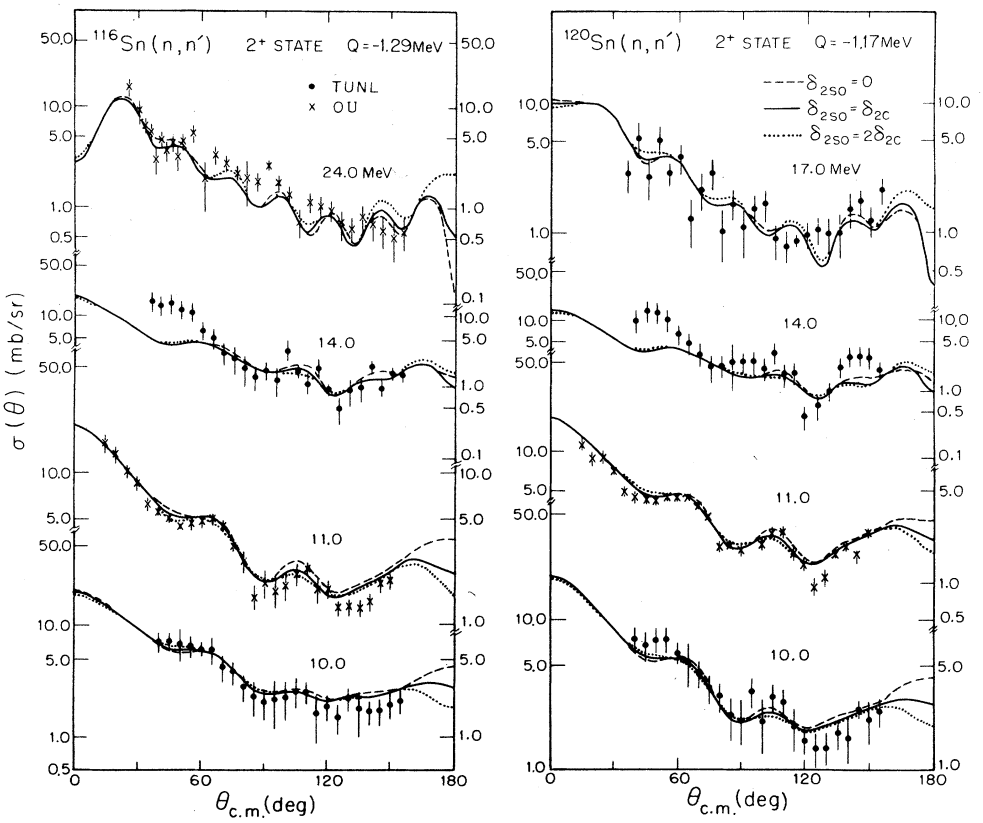

FIG. 3. Differential cross sections for neutron inelastic scattering from the first 2$^+$ state of ^{116}Sn and ^{120}Sn. For other comments see Fig. 2.

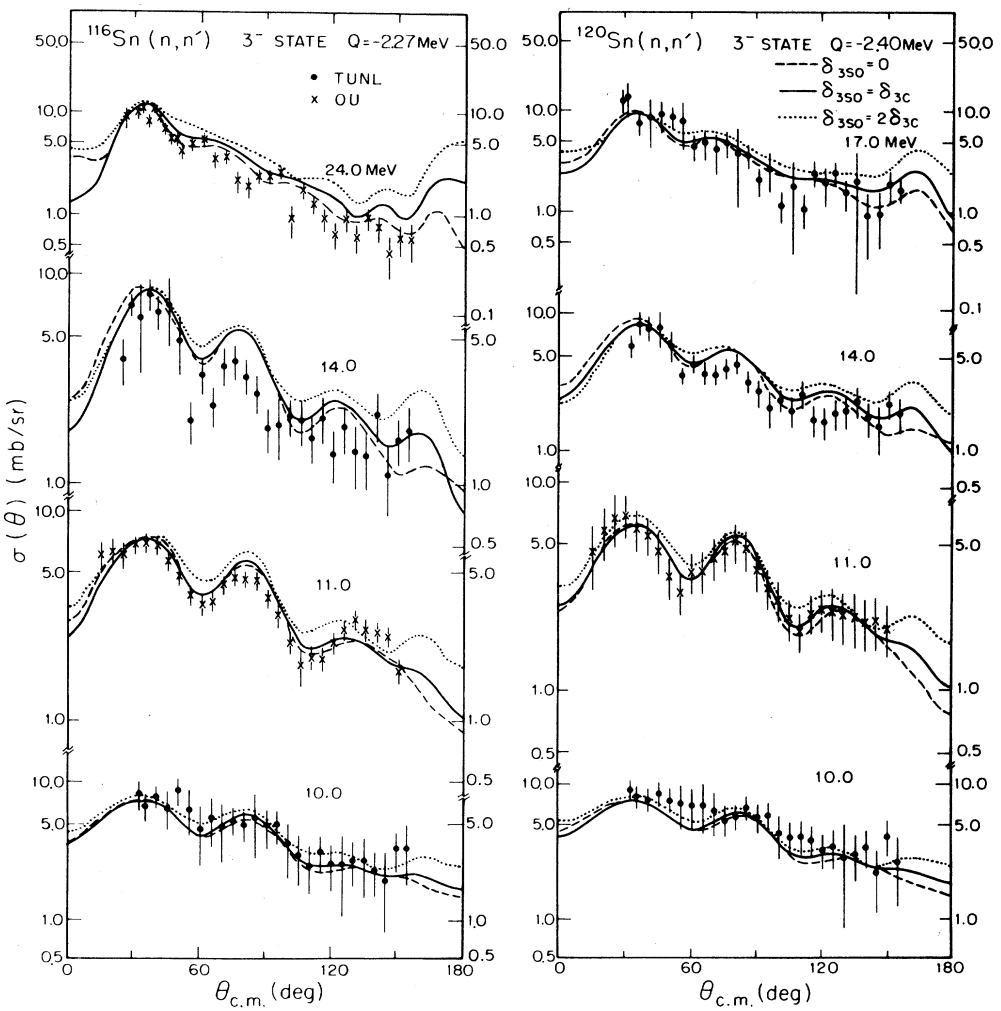

FIG. 4. Differential cross sections for neutron inelastic scattering from the first 3^- state of ^{116}Sn and ^{120}Sn. For other comments, see Fig. 2. The calculations include small contributions from neighboring levels not resolved in the present measurements (see the text).

that the model parameters were somewhat physically meaningful within this energy range was made by conducting a calculation of $\sigma(\theta)$ for ^{116}Sn(n,n) at 1.63 MeV and comparing to the work of Harper *et al.*[39] When the compound-nucleus contribution reported in Ref. 39 was added to our CC calculation, the shape was fairly well predicted. That is, the calculation agreed with their data to within ±20% and the single minimum in the $\sigma(\theta)$ data, which occurs near 115°, was properly predicted.]

IV. COMPARISON OF DEFORMATIONS OBTAINED FROM (n,n') AND (p,p') SCATTERING

An investigation was also conducted mainly to determine whether the quadrupole deformation lengths $\delta^{2^+}_{nn'}$ from (n,n') scattering are smaller than the $\delta^{2^+}_{pp'}$ from (p,p') scattering, as expected for the $Z=50$ isotopes from the calculations in the core-polarization model of Brown *et al.*[40] A second motivation for this study was to extract $\delta^{3^-}_{pp'}$ values for octupole vibrations and to compare them to $\delta^{3^-}_{nn'}$ values for ^{116}Sn and ^{120}Sn. The latter was done even though we knew that the task is more difficult than it is for the quadrupole vibration because in the present (n,n') measurements the low-lying 3^- states could not be resolved from neighboring states (see Sec. II). An additional reason that makes this latter comparison more delicate for ^{120}Sn is that an excited state has not been resolved from the first 3^- state in the (p,p') measurements of Makofske *et al.*[3] at 16 MeV. In contrast with the assumption made there that this state is the 4^+ level lying at an excitation energy of 2.19 MeV, we presume this state is the 4^+ level at 2.46 MeV. (See Ref. 26 and Fig. 1.)

The (p,p) and (p,p') calculations presented here have been conducted in a manner similar to that explained in considerable detail in Ref. 11. Therefore, only the important points will be mentioned here. The first one deals with the coupling scheme, which involves levels with spins and parities identical to those assumed in Sec. III for ^{116}Sn and ^{120}Sn. However, as already stated, the exci-

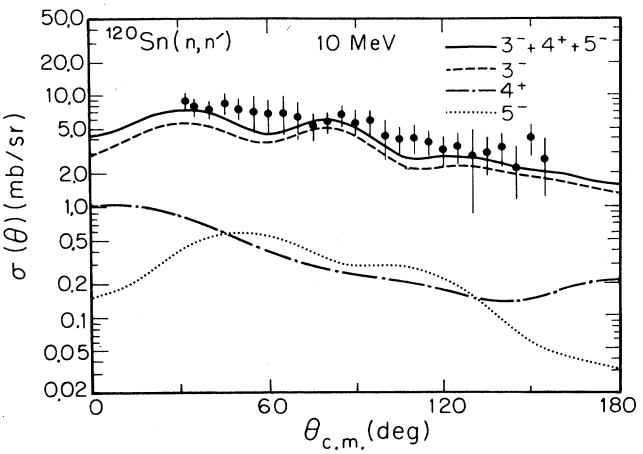

FIG. 5. Inelastic scattering to the unresolved multiplets in the vicinity of the first octupole state of ^{120}Sn. It is shown how direct interaction contributions from individual collective states combine altogether to represent the present measurement at 10 MeV. In the CC calculations it was assumed that the deformation lengths for the central and spin-orbit potentials were identical.

tation energy that we assumed for the 4^+ state of ^{120}Sn is 2.46 MeV instead of 2.19 MeV. This substitution was made in order to carefully analyze the (p,p') scattering measurements[3] for the 3^- state of ^{120}Sn while avoiding part of the ambiguities tied with adopting a coupling scheme for this nucleus that would include two 4^+ levels. The deformation length δ_{4c} adopted for the 4^+ (2.46-MeV) state was inferred from Ref. 27.

The optimum fits to the (p,p) and (p,p') scattering measurements at 16 MeV were obtained with the following potential depths:

$$V = 51.97 - 0.22E + 20.83\epsilon + \Delta V_C$$

and

$$W_D = 3.29 + 1.71\sqrt{E} + 15.97\epsilon + \Delta W_C \ .$$

The potential was written in this form to make it isospin consistent with the neutron potential. The strengths and energy dependences of the first two terms in each potential are identical to the neutron case and the symmetry terms have identical magnitudes. (See Table II.) The so-called Coulomb correction term ΔV_C of the real potential

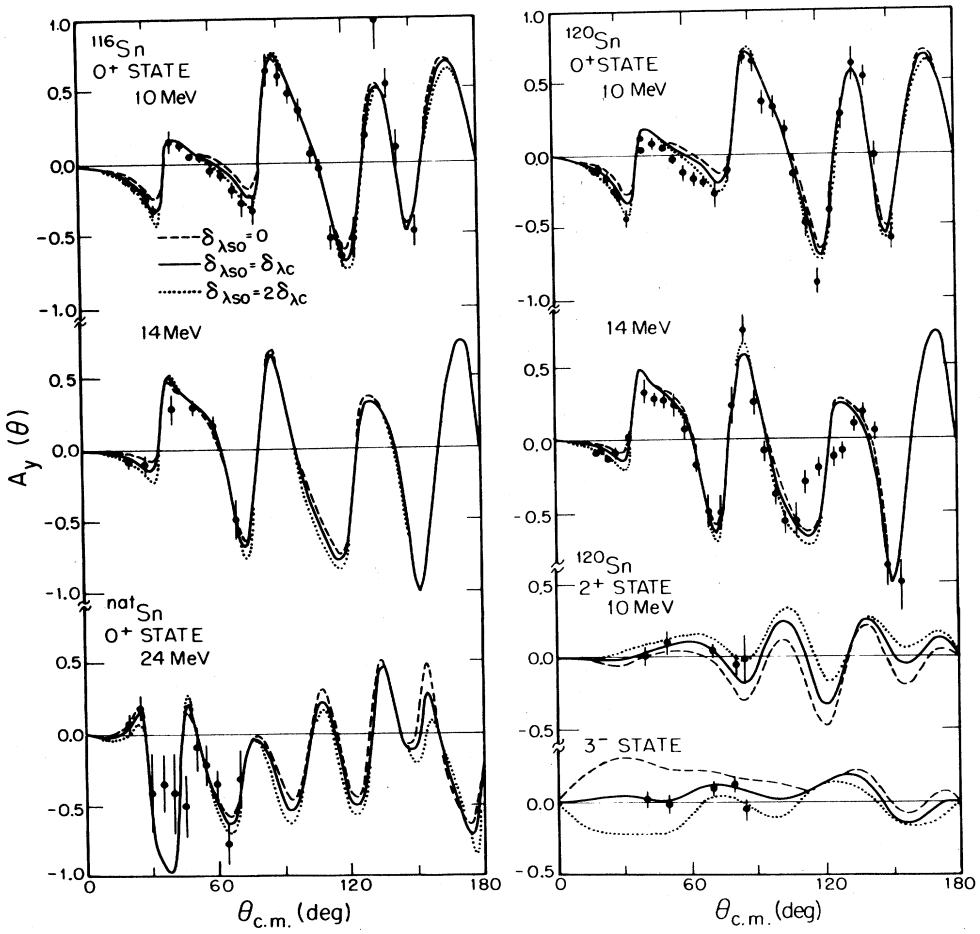

FIG. 6. Analyzing powers for neutron elastic and inelastic scattering from ^{116}Sn, ^{120}Sn, and ^{nat}Sn. The data at 24 MeV are from Ref. 37; the other data have been obtained in the present experiment. The curves shown for the 3^- state are obtained by folding in contributions from unresolved states (see the text). The dotted, dashed, and solid curves represent CC calculations in which δ_{2SO} and δ_{3SO} are varied.

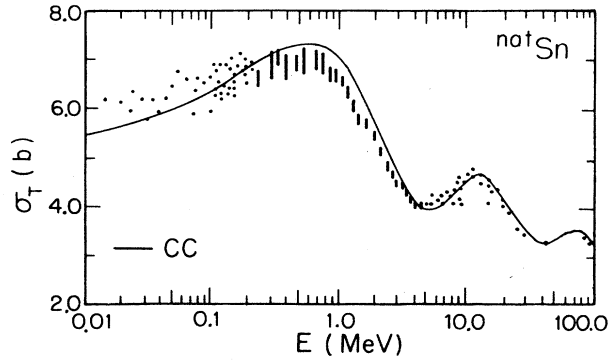

FIG. 7. Total neutron cross section of Sn between 10 keV and 100 MeV. The data shown for 0.25 MeV $< E <$ 4.50 MeV are from Ref. 6 and the others are from Ref. 5. The solid curve represents CC calculations of the present work (see the text).

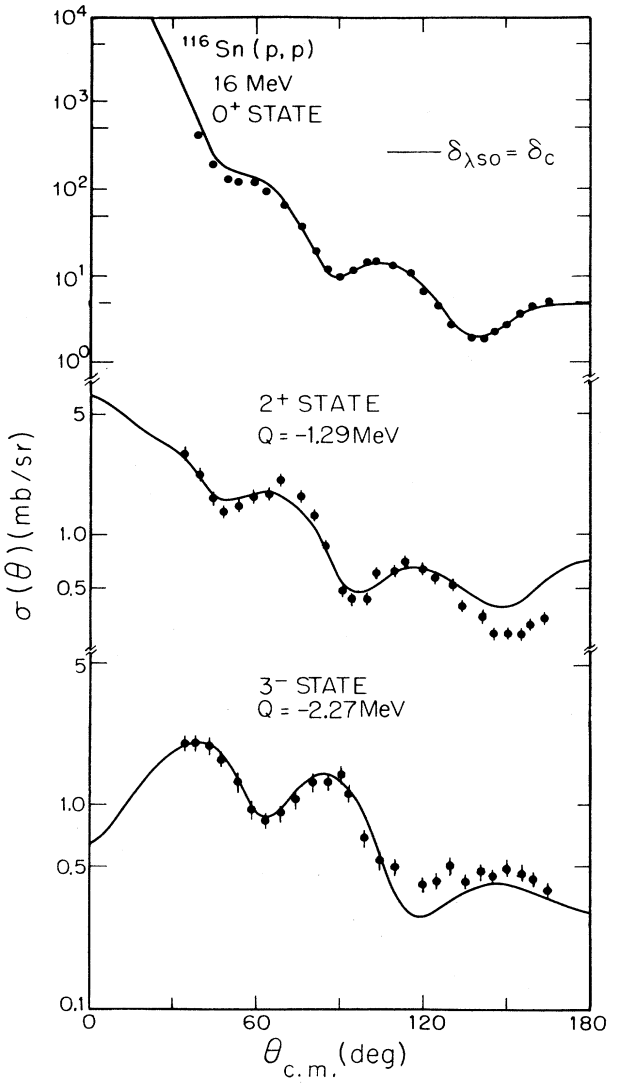

FIG. 8. Elastic and inelastic scattering of 16-MeV protons from ^{116}Sn. The comparison is between the measurements of Ref. 3 and present CC calculations.

was assigned the usual value of 0.4 $Z/A^{1/3}$ MeV and ΔW_C of the imaginary potential was found to favor a value of $\Delta W_C = -0.5$ MeV, although the uncertainty on ΔW_C was found to be large, i.e., about 50%. For $\delta_{\lambda SO}$ (with $\lambda=2,3$) we have adopted the values $\delta_{\lambda SO}=\delta_{\lambda c}$ inferred from Ref. 19 and present sensitivity calculations. For $\delta_{\lambda SO}$ with ($\lambda=4,5$) we have also assumed that $\delta_{\lambda SO}=\delta_{\lambda c}$. An illustration of the results of the present CC analysis is given in Fig. 8 for ^{116}Sn. Reasonably good agreement between the calculations and the measurements is achieved. This is also the case for ^{120}Sn, although the comparison is not shown here.

The deformation β_λ^V and deformation lengths $\delta_{\lambda c}$ of the real central potential for quadrupole and octupole transitions obtained from our proton scattering analyses are shown in Table II. Although the uncertainties are relatively large (see Table II), the comparison in Table II between the quadrupole vibration amplitudes deduced from (n,n') and (p,p') measurements suggests that the relation $\delta_{nn'}^{2^+} \leq \delta_{pp'}^{2^+}$ proposed by Brown and Madsen[40] holds for the $Z=50$ isotopes. On the other hand, our analysis suggests that $\delta_{nn'}^{3^-} \cong \delta_{pp'}^{3^-}$ for octupole vibrations. Unfortunately, calculations in the core polarization model[40] do not exist yet for octupole transitions in Sn. Finally, the empirical findings about the deformation lengths that we derived in the CC analysis of the comprehensive set of data are consistent with DWBA results for Sn nuclei published by Finlay *et al.*[2] The deformation parameters obtained above in the analysis of the proton data of Makofske *et al.*[3] overlap with the values reported by Abbott *et al.*[41] in an analysis of recently obtained proton data at 16 MeV. This latter analysis was based in part on the present neutron analysis, so the values of Abbott *et al.* should not be considered completely independent of those reported here, however.

V. COMMENTS ABOUT $W_V(E)$ AND W_{SO}

The volume integrals for the real and imaginary potentials (J_V/A and J_W/A, respectively) deduced from our CC analysis were calculated and compared to those for the microscopic model of Jeukenne, Lejeune, and Mahaux,[42,43] denoted by JLM. The calculations for J_V/A for our CC model agree with the JLM values to within 3% over the entire energy range. A similar comparison for J_W/A is not as straightforward since the JLM calculations[42] of the absorptive potential are based on a spherical model, whereas an absorptive potential derived from microscopic CC calculations would be lower in magnitude due to the absorption processes that are explicitly accounted for in the CC method. We note that J_W/A for our CC model falls about 15% to 25% under that of JLM in the energy range between 10 and 30 MeV. Considering our coupling scheme and some phenomenological spherical optical model calculations that were performed by us,[20] a decrease of this percentage is reasonable. However, the CC values for J_W/A cross over the JLM values around 50 MeV and by 100 MeV exceed the JLM values by 25%. This apparently unphysical behavior, in relation to the JLM predictions, can be eliminated

by allowing the W_V to fall off to a nearly constant value for neutron energies above about 60 MeV. Such energy dependences are being investigated now at TUNL (Ref. 44) in a renewed attempt to describe neutron scattering data for Ni and Fe isotopes from 10 keV to 80 MeV.

It was stated above that we chose to set $W_{SO}=0$ for the present analysis. The importance of this term has not been carefully explored for nucleon-nucleus scattering in the energy range below 30 MeV, particularly in the CC method. From the proton-nucleus analysis of Schwandt *et al.*,[45] the spherical optical model prefers a W_{SO} that is negative around 80 MeV and above, and that is probably near zero around 50 MeV. In the phenomenological spherical optical model studies of the $A_y(\theta)$ for neutron-nucleus scattering around 10 MeV that are being conducted at TUNL, some analyses favor a W_{SO} that is positive. Inclusion of a nonzero W_{SO} in the CC calculations affects $A_y(\theta)$ for both elastic and inelastic scattering, and leads to ambiguities between δ_{SO} and W_{SO}. It would be helpful to have better quality $\sigma(\theta)$ and $A_y(\theta)$ data for inelastic scattering, as well as additional $A_y(\theta)$ data for elastic scattering over a wider neutron energy range in order to characterize the nature of W_{SO} below 30 MeV.

VI. CONCLUDING REMARKS

The aim of the present $\sigma(\theta)$ and $A_y(\theta)$ measurements was to obtain information about the scattering properties of ^{116}Sn and ^{120}Sn in the energy interval from 10 to 17 MeV. These measurements, as well as earlier results that include differential and total cross sections and strength functions, have been combined to develop a phenomenological, deformed optical potential for the whole energy range from 10 keV to 100 MeV. The potential parameters are listed in Table I.

First, the geometrical parameters and well depths determined here for the spin-orbit (SO) potential are somewhat similar to those derived[33] earlier in this laboratory for Fe and Cu. Second, the SO potential must be deformed in order to reproduce the $A_y(\theta)$ data for (n,n') scattering. Under the assumption that there is no imaginary SO potential, the deformation lengths for the central and SO terms of the optical potential are found to be nearly identical. These results are at variance with earlier conjectures,[7] which suggest that $\delta_{SO}\cong 2\delta_c$ for quadrupole transitions induced by (n,n') scattering from proton closed-shell nuclei.

Our deformed optical potential is energy dependent and includes a symmetry term. At very low incident energy ($E\cong 10$ keV) the small values of W_D directly reflect the very small S_0 values measured previously for the s-wave strength functions. A steep increase of W_D is required in the interval 10 keV $< E \leq$ 10 MeV. This empirical finding is consistent with the microscopic spherical optical model predictions of JLM for 2 MeV $\leq E \leq$ 10 MeV. For $E \geq 10$ MeV the volume and surface absorptions have a strong interplay; the surface absorption was found to vanish at about 100 MeV. However, about equally good fits of the σ_T data can be obtained with a combination of a W_D that drops linearly to zero around 70 MeV and a W_V that has a steeper slope and flattens out around 80 MeV. Differential cross-section and $A_y(\theta)$ data for neutron scattering in the 50- to 70-MeV energy range would provide useful information for constraining the parameters more tightly in this region. Some ambiguity still exists at low energies also. In our model we chose to allow the strength of W_V to approach zero linearly. The data favored the occurrence of this intercept at 13 MeV. However, if instead W_V is allowed to approach zero asymptotically, the data do not rule out a W_V of about 0.5 MeV around an incident energy of 10 MeV, if W_D is allowed to decrease correspondingly.

The criterion employed in the present analysis for obtaining the best overall fit was the best qualitative agreement, in our judgment. Of course, this method of evaluation is quite subjective. Therefore, limits on the range of most parameters have not been stated here. As indicated above, different functional forms of energy dependences will give new families of potentials. The present potential is clearly not unique; however, within the constraints expressed above, it does give a good description of a wealth of data. We have refrained from defining limits on the range of the W_D and W_V parameters using the usual standard of chi squared per degree of freedom. This measure is hard to interpret because different groups use different criteria for assigning uncertainties to the data, and because weaknesses in the model cause systematic discrepancies in $\sigma(\theta)$ or $A_y(\theta)$ in certain angular regions.

The symmetry potential $U_1=V_1+iW_{D1}$, with $V_1\cong 21$ MeV and $W_{D1}\cong 16$ MeV, is consistent with the isotopic differences existing between the interaction of neutrons with ^{116}Sn and ^{120}Sn. An anomalously large W_{D1} value was not found to be required in the present analysis. Our estimated value $W_{D1}=(16\pm 5)$ MeV is intermediate between the values of 12 and 23 MeV found in earlier independent (n,n') and (p,p') scattering studies, respectively. It is also consistent with the average value of 16.6 MeV obtained by Wong *et al.*[46] in an isospin-consistent spherical optical model analysis of differential cross-section data for elastic nucleon scattering and for the analog-state (p,n) reaction at 25 MeV for Sn.

ACKNOWLEDGMENTS

We are grateful to C. E. Floyd, K. Murphy, G. Honoré, and H. Pfützner who assisted at various stages of the measurements and to Dr. J. H. Davé for providing the JLM volume integral predictions. We also appreciate the cooperation of Dr. D. C. Larson and Dr. J. A. Harvey in allowing us to compare our calculations to their unpublished total cross-section measurements. Lastly, we thank Dr. A. Lejeune for informative discussions regarding the properties of the imaginary potential at high energies. This work was supported in part by the U.S. Department of Energy, Office of High Energy and Nuclear Physics, under Contract No. DE-AC05-76ER01067.

*Present address: EG&G Energy Measurements, Andrews AFB, Washington, D.C.
†Present address: Physics Division, Los Alamos National Laboratory, Los Alamos, NM 87545.
‡Present address: Department of Physics, University of Ohio, Athens, OH 45701.
§Present address: Department of Physics, University of Birmingham, Birmingham, England.

[1]J. Rapaport, M. Mirzaa, H. Hadizadeh, D. E. Bainum, and R. W. Finlay, Nucl. Phys. **A341**, 56 (1980).
[2]R. W. Finlay, J. Rapaport, M. H. Hadizadeh, M. Mirzaa, and D. E. Bainum, Nucl. Phys. **A338**, 45 (1980); R. W. Finlay, M. H. Hadizadeh, J. Rapaport, and D. E. Bainum, *ibid.* **A344**, 257 (1980).
[3]W. Makofske, W. Savin, H. Ogata, and T. H. Kruse, Phys. Rev. **174**, 1629 (1968).
[4]S. F. Mughabghab and D. I. Garber, Brookhaven National Laboratory Report No. BNL-325, 1973, 3rd ed., Vol. I.
[5]D. I. Garber and R. R. Kinsey, BNL Report No. BNL-325, 1976, 3rd ed., Vol. II.
[6]C. Budtz-Jorgensen, P. Guenther, and A. B. Smith, Argonne National Laboratory Report No. ANL/NDM-73, 1982.
[7]J. Raynal, International Atomic Energy Agency Report No. IAEA-SMR-9/8, 1972, p. 75.
[8]C. Shakin, Ann. Phys. (N.Y.) **22**, 373 (1963).
[9]B. Buck and F. Perey, Phys. Rev. Lett. **8**, 444 (1962); D. M. Chase, L. Wilets, and A. R. Edmonds, Phys. Rev. **110**, 1080 (1958).
[10]C. M. Newstead, J. P. Delaroche, and B. Cauvin, in *Statistical Properties of Nuclei,* edited by J. B. Garg (Plenum, New York, 1972), p. 367; C. M. Newstead and J. P. Delaroche, in *Nuclear Structure Study with Neutrons* (Plenum, New York, 1974), p. 142.
[11]J. P. Delaroche, S. M. El-Kadi, P. P. Guss, C. E. Floyd, and R. L. Walter, Nucl. Phys. **390**, 541 (1982), and references therein.
[12]J. Rapaport, contribution to the Symposium on Isospin Effects in Nuclear Structure, Oregon State University, 1985 (unpublished); F. D. Becchetti and G. W. Greenlees, Phys. Rev. **182**, 1190 (1969).
[13]J. D. Carlson, C. D. Zaffiratos, and D. A. Lind, Nucl. Phys. **A249**, 29 (1975); D. M. Petterson, R. R. Doering, and Aaron Galonsky, *ibid.* **A263**, 261 (1976).
[14]F. S. Dietrich, R. W. Finlay, S. Mellema, G. Randers-Pehrson, and F. Petrovich, Phys. Rev. Lett. **51**, 1629 (1983).
[15]Ch. Lagrange and A. Lejeune, Phys. Rev. C **25**, 2278 (1982).
[16]S. H. Mellema, R. W. Finlay, F. S. Dietrich, and F. Petrovich, Phys. Rev. C **28**, 2267 (1983).
[17]C. H. Johnson, D. J. Horen, and C. Mahaux, Phys. Rev. C **36**, 2252 (1987), and references therein.
[18]J. P. Delaroche and W. Tornow, Phys. Lett. B **203**, 4 (1988).
[19]P. P. Guss, C. E. Floyd, K. Murphy, C. R. Howell, R. S. Pedroni, G. M. Honoré, H. G. Pfützner, G. Tungate, R. C. Byrd, R. L. Walter, and J. P. Delaroche, Phys. Rev. C **25**, 2854 (1982), and references therein.
[20]P. P. Guss, Ph.D. thesis, Duke University, 1982, available from University Microfilms, Ann Arbor, MI.
[21]S. M. El-Kadi, C. E. Nelson, F. O. Purser, R. L. Walter, A. Beyerle, C. R. Gould, and L. W. Seagondollar, Nucl. Phys. **A390**, 509 (1982).
[22]P. P. Guss, R. C. Byrd, C. E. Floyd, C. R. Howell, K. Murphy, G. Tungate, R. S. Pedroni, R. L. Walter, and J. P. Delaroche, Nucl. Phys. **A438**, 187 (1985).
[23]S. A. Wender, C. E. Floyd, T. B. Clegg, and W. R. Wylie, Nucl. Instrum. Methods **174**, 341 (1980); C. R. Howell and S. A. Wender, *ibid.* **195**, 443 (1982).
[24]P. W. Lisowski, R. L. Walter, C. E. Busch, and T. B. Clegg, Nucl. Phys. **A242**, 298 (1975).
[25]J. P. Delaroche, Ch. Lagrange, and J. Salvy, in *Nuclear Theory in Neutron Nuclear Data Evaluation* (IAEA, Vienna, 1976), Vol. II, p. 251.
[26]*Table of Isotopes,* 7th ed., edited by C. M. Lederer and V. S. Shirley (Wiley, New York, 1978).
[27]O. Beer, A. El Behay, P. Lopato, Y. Terrien, G. Vallois, and K. K. Seth, Nucl. Phys. **A147**, 326 (1970).
[28]J. Bron *et al.*, Nucl. Phys. **A318**, 335 (1979); I. Morrison and R. Smith, *ibid.* **A350**, 89 (1980).
[29]A. Christy and O. Hausser, Nucl. Data Tables **11**, 281 (1972).
[30]T. Tamura, Rev. Mod. Phys. **37**, 679 (1965).
[31]H. Sherif and J. S. Blair, Phys. Lett. **26B**, 489 (1968); J. Raynal, International Atomic Energy Agency Report No. IAEA-SMR-818, 1972, p. 75.
[32]J. P. Delaroche, P. P. Guss, C. E. Floyd, R. L. Walter, and W. Tornow, Phys. Rev. C **27**, 2385 (1983).
[33]C. E. Floyd, P. P. Guss, R. C. Byrd, K. Murphy, R. L. Walter, and J. P. Delaroche, Phys. Rev. C **28**, 1498 (1983).
[34]J. Raynal, in *Computing as a Language of Physics* (IAEA, Vienna, 1972).
[35]J. Schwinger, Phys. Rev. **73**, 407 (1948).
[36]S. F. Mughabghab, M. Divadeenam, and N. E. Holden, in *Neutron Cross Sections* (Academic, New York, 1981).
[37]C. Wong, J. D. Anderson, J. W. McClure, and B. D. Walker, Phys. Rev. **128**, 2339 (1962).
[38]D. C. Larson and J. A. Harvey, private communication.
[39]R. W. Harper, J. L. Weil, and J. D. Brandenberger, Phys. Rev. C **30**, 1454 (1984).
[40]V. R. Brown and V. A. Madsen, Phys. Rec. C **11**, 1298 (1975); V. A. Madsen, V. R. Brown, and J. D. Anderson, *ibid.* **12**, 1205 (1975).
[41]D. J. Abbott, T. B. Clegg, and J. P. Delaroche, Phys. Rev. **35**, 2028 (1987).
[42]J. P. Jeukenne, A. Lejeune, and C. Mahaux, Phys. Rev. C **16**, 80 (1977); A. Lejeune, *ibid.* **21**, 1107 (1980).
[43]J. W. Negele and K. Yazaki, Phys. Rev. Lett. **47**, 71 (1981); S. Fantoni, B. L. Friman, and V. R. Pandharipande, Phys. Lett. **104B**, 89 (1981).
[44]This investigation, which is being carried out by two of the present authors (C.R.H. and J.P.D.), is a followup of the report by R. S. Pedroni *et al.* in Phys. Rev. C **38**, 2052 (1988).
[45]P. Schwandt, H. O. Meyer, W. W. Jacobs, A. D. Bacher, S. E. Vigdor, M. D. Kaitchuck, and T. R. Donoghue, Phys. Rev. C **26**, 55 (1982).
[46]C. Wong, S. M. Grimes, and R. W. Finlay, Phys. Rev. C **29**, 1710 (1984).